AD-A162 036

DTIC ACCESSION NUMBER

LEVEL

INVENTORY

①

DESIGN AND ANALYSIS OF CONTROL LAWS
FOR THE VERTICAL SEEKING SEAT
AND THE MICRAD ATTITUDE REFERENCE SYSTEM

DOCUMENT IDENTIFICATION

DISTRIBUTION STATEMENT A
Approved for public release
Distribution Unlimited

DISTRIBUTION STATEMENT

ACCESSION FOR	
NTIS GRA&I	✓
DTIC TAB	☐
UNANNOUNCED	☐
JUSTIFICATION	

PER LETTER

BY	
DISTRIBUTION /	
AVAILABILITY CODES	
DIST	AVAIL AND/OR SPECIAL

A-1

DISTRIBUTION STAMP

QUALITY INSPECTED 3

DTIC FILE COPY

DTIC
ELECTE
DEC 2 1985
S D
B

DATE ACCESSIONED

DATE RETURNED

85 09 04 048

DATE RECEIVED IN DTIC

REGISTERED OR CERTIFIED NO.

DTIC FORM 70A
DEC 83

DOCUMENT PROCESSING SHEET

PREVIOUS EDITION MAY BE USED UNTIL
STOCK IS EXHAUSTED.

DESIGN AND ANALYSIS OF CONTROL LAWS
FOR THE VERTICAL SEEKING SEAT
AND THE MICRAD ATTITUDE REFERENCE SYSTEM

4 APRIL 1980

AD-A162 036

Systems Analysis
& Control

Specializing in Analysis & Control of Dynamic Systems

85 09 04 04 8

DESIGN AND ANALYSIS OF CONTROL LAWS
FOR THE VERTICAL SEEKING SEAT
AND THE MICRAD ATTITUDE REFERENCE SYSTEM

4 APRIL 1980

SUMMARY

One problem with using the MICRAD Attitude Reference System (MARS) to provide error signals to the Vertical Seeking Seat (VSS) control system is that the MARS outputs vary significantly depending on whether the local earth's surface is land or water. This variation changes the control system gain resulting in degraded performance. As a result, efforts were initiated to develop alternatives and/or improvements to control laws studied previously at the Naval Weapons Center (NWC). An alternate control law was developed and evaluated using a digital simulation. Results indicated that this control law provided good performance and adequately compensated for variations in the MARS outputs.

ii

TABLE OF CONTENTS

INTRODUCTION

The Maximum Performance Ejection Seat (MPES) or Vertical Seeking Seat (VSS) escape system requires a vertical reference to provide commands for the control system. Previous tests of the MPES/VSS system were performed using a strap-down vertical reference system which was initialized at the planned "launch" attitude. Although this attitude hand-off is satisfactory for initial tests, the operational system should use an autonomous reference system. One such system which is to be used in future flight tests is the Micro-wave Radiometric (MICRAD) Attitude Reference System (MARS).

The MARS contains a reference load and four antennas which measure the natural radiation emanating from objects within their field of view, such as the earth or sky or combinations of the two. The outputs of the MARS are an indication of the relative temperatures of the load and those sensed by each antenna. These four measures of relative temperature are to be processed by control laws whose outputs are used to drive angular velocity feedback control loops. One area of concern is that the significant difference between the microwave temperatures of land and water may change the gain of the control laws, thus making the system response dependent upon the local make-up of the earth's surface.

The objective of this effort is to develop alternatives and improvements to control laws studied previously at the Naval Weapons Center (NWC). Specifically, the problem of compensating for the different temperatures of land and water will be addressed. The resulting control laws are to be suitable for implementation in the on-board microprocessor. Although the candidate control laws need not be optimized for all flight conditions, they will be evaluated for several flight conditions using a six Degree of Freedom program provided by NWC.

CANDIDATE CONTROL LAWS

Three control laws have previously been studied at NWC for use with the MARS. These laws and their origin are briefly discussed here for completeness. In the case of the Heuristic Control Law, an attempted derivation yielded a modified control law which is also considered as a candidate.

DIRECTION COSINE CONTROL LAW

The Direction Cosine Control Law (DCCL) is based on commanding body angular velocities, q and p, proportional to the cosines of the angles between the nadir and the x and y body axes respectively. One method of viewing and implementing the DCCL with the MARS outputs is shown here. Consider the component of a vector, representing the temperature difference between the nadir and zenith, in the seat body x - y plane as shown in Figure 1. When the seat is aligned with the vertical, the vector component ΔT is zero. This suggests that the

$\hat{x} - \hat{y}$ Body Axes

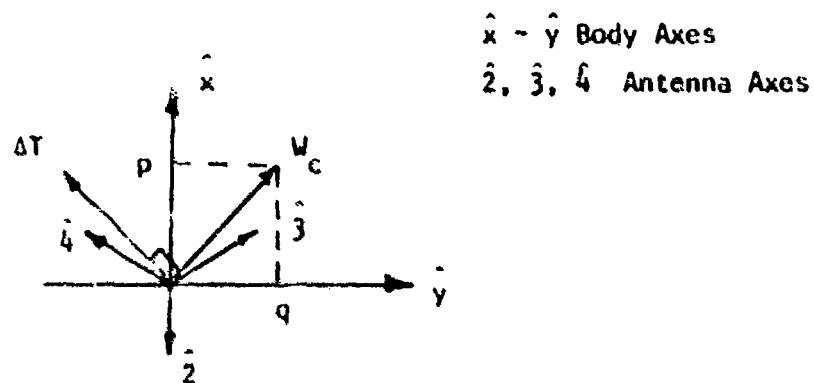$\hat{2}, \hat{3}, \hat{4}$ Antenna Axes

FIGURE 1. Seat Body x - y Plane Showing Temperature Difference and Desired Angular Velocity.

seat be rotated about an axis perpendicular to ΔT in the x - y plane. Thus the commanded angular velocity, shown in Figure 1, can be expressed in terms of ΔT.

If

$$\Delta T = q \hat{x} - p \hat{y}$$

then

$$W_c = p \hat{x} + q \hat{y}$$

(1)

2

In order to obtain p and q as functions of the antenna outputs, we must determine components of ΔT along the antenna axes.

$$a_2 = - q \; \hat{2}$$

$$a_3 = (q \cos 60° - p \cos 30°) \; \hat{3} \qquad\qquad (2)$$

$$a_4 = (q \cos 60° + p \cos 30°) \; \hat{4}$$

These equations can be rearranged to yield

$$p = \frac{a_4 - a_3}{\sqrt{3}}$$

$$\qquad\qquad (3)$$

$$q = \frac{a_3 + a_4 - a_2}{2}$$

which define the commanded angular velocity in body axes in terms of the _normalized_ antenna outputs a_i. It was shown in Reference 1 that if the normalized antenna outputs a_2, a_3, and a_4 are cosines of the angles between the respective antenna and the nadir, then Equation (3) is equivalent to the DCCL if p and q are the commanded roll and pitch rates respectively. In general this will _not_ be the case since the antenna outputs will _not_ be normalized to a cosine function. Therefore, Equation (3) will be referred to as the MARS Direction Cosine Control Law (MDCCL).

HEURISTIC AND MODIFIED HEURISTIC CONTROL LAW

The Heuristic Control Law (HCL) is

$$p = a_4 - a_3$$

$$\qquad\qquad (4)$$

$$q = \frac{a_3 + a_4}{2} - a_2$$

where p and q are the commanded angular velocities and the antenna outputs a_2, a_3, and a_4 are considered to be normalized. An expression very similar to Equation (4) can be obtained by resolving the antenna outputs into the x and y body axes.

3

From Figure 1

$$a_x = (-a_2 + a_3 \sin 30° + a_4 \sin 30°) \, \hat{x}$$

$$a_y = (a_3 \cos 30° - a_4 \cos 30°) \, \hat{y}$$

or

$$a_x = (\frac{a_3 + a_4}{2} - a_2) \, \hat{x}$$

$$a_y = [\frac{\sqrt{3}}{2} (a_3 - a_4)] \, \hat{y}$$

Now define the commanded angular velocity as

$$W_c = -a_y \, \hat{x} + a_x \, \hat{y}$$

$$= p \, \hat{x} + q \, \hat{y}$$

or

$$p = \frac{\sqrt{3}}{2} (a_4 - a_3)$$

$$q = \frac{a_3 + a_4}{2} - a_2$$

(5)

Note that Equations (4) and (5) differ by a constant factor in the expression for p. Therefore, Equation (5) will also be considered as a candidate control law and will be referred to as the Modified Heuristic Control Law (MHCL).

PERMUTATION CONTROL LAW

The Permutation, or table look-up, Control Law (PCL) is based on sorting the four MARS antenna outputs in order of coldest to warmest and using predetermined angular velocity commands for each permutation of the antenna outputs. Since the resolution of the resulting on-off control logic is significantly less than the desired system accuracy, additional proportional control logic is required when the seat is near its desired attitude. A detailed description of the PCL can be found in Reference 1.

ANALYSIS OF CONTROL LAWS

Each of the previously described control laws is briefly analyzed. Initially, the proportional control laws, that is, the Direction Cosine, Heuristic, and Modified Heuristic Laws are evaluated with regard to their characteristics using un-normalized antenna outputs with varying nadir temperatures. Next, the error between the commanded angular velocity axis defined by each of the control laws is compared with an axis which minimizes the rotation angle required to align the seat with the vertical. Finally, a similar comparison of the permutation law commands with those required for a minimal rotation axis is made. Based on this analysis, a control law is selected for further evaluation using the NWC six Degree of Freedom (DOF) digital simulation.

EFFECTS OF MARS OUTPUT CHARACTERISTICS

As discussed previously, the MARS antennas measure temperature and, therefore, their outputs are significantly dependent on whether the sensor is over land or water. This causes large gain or scale factor variations in the proportional control laws, if un-normalized antenna outputs are used directly, which may degrade the system response. One solution to this problem is to normalize the antenna outputs. However, this may be difficult since the nadir and zenith temperatures are not known a priori and may not both be measured, depending on the seat trajectory. Insight is obtained by evaluating the control laws using an expression for the normalized antenna outputs in terms of the actual outputs. Assume that the actual output of an antenna at the horizon $\bar{A}$ is the average of the actual outputs of antennas pointing at the nadir A_n and zenith A_z.

$$\bar{A} = \frac{A_n + A_z}{2} \tag{6}$$

Now, assuming MARS outputs high (low) voltages for low (high) temperatures, define the normalized output a_i of antenna i as

$$a_i = \frac{A_i - \bar{A}}{A_z - \bar{A}} \tag{7}$$

5

Where A_i is the actual output of antenna i. Substituting Equation (6) into (7) and rearranging yields

$$a_i = \frac{2A_i - (A_n + A_z)}{A_z - A_n} \qquad (8)$$

The normalized antenna outputs defined by Equation (8) are used directly in the MDCCL and HCL, that is, in Equations (3) and (4) respectively. The resulting MDCCL is

$$p = \frac{2(A_4 - A_3)}{(A_z - A_n)\sqrt{3}} \qquad (9)$$

$$q = \frac{2(A_3 + A_4 - A_2) - (A_n + A_z)}{2(A_z - A_n)}$$

and the HCL is

$$p = \frac{2}{A_z - A_n}(A_4 - A_3)$$

$$\qquad (10)$$

$$q = \frac{2}{A_z - A_n}\left(\frac{A_3 + A_4}{2} - A_2\right)$$

The MHCL is not listed as it is very similar to the HCL. Note that in Equations (9) and (10), A_2, A_3, and A_4 are the un-normalized antenna outputs and therefore these equations will be referred to as un-normalized control laws.

A comparison of Equations (4) and (10) indicates the normalized and un-normalized HCL's are related by a factor of $2/(A_z - A_n)$. The relationship of the corresponding MDCCL's, Equations (3) and (9), is somewhat more complicated. Implementation of Equations (9) and (10) requires knowledge of $(A_z - A_n)$ and the former also requires knowledge of $(A_n + A_z)$. As mentioned previously, the exact values of A_n and A_z are not known a priori. However, it may be possible to estimate them using the fact that A_z is relatively constant under varying meteorological conditions. Thus the use of a predetermined

6

constant to approximate A_z may be feasible. Also helpful is the following approximation for the actual output of an antenna pointing at the horizon.

$$\bar{A} \simeq \frac{A_2 + A_3 + A_4}{3} \tag{11}$$

Equation (6) can be rearranged to yield

$$A_n + A_z = 2\,\bar{A} \tag{12}$$

where $\bar{A}$ is obtained using Equation (11). Now Equation (12) can be used along with a predetermined estimate of A_z, designated as $\hat{A}_z$, to provide

$$A_z - A_n = 2\,(\hat{A}_z - \bar{A}) \tag{13}$$

where $\bar{A}$ is again obtained using Equation (11). Equations (11), (12), and (13) can be used to estimate the quantities required for implementation of the un-normalized control laws as follows. The HDCCL is now

$$p = \frac{(A_4 - A_3)}{(\hat{A}_z - \bar{A})\;\sqrt{3}} \tag{14}$$

$$q = \frac{(A_3 + A_4 - A_2) - \bar{A}}{2(\hat{A}_z - \bar{A})}$$

and the HCL is

$$p = \frac{A_4 - A_3}{\hat{A}_z - \bar{A}} \tag{15}$$

$$q = \frac{1}{\hat{A}_z - \bar{A}}\;\left(\frac{A_3 + A_4}{2} - A_2\right)$$

where $\bar{A}$ is defined by Equation (11). The HHCL is the same as Equation (15) except the former has an additional factor of $\sqrt{3}/2$ in

7

the expression for p. The effectiveness of the above approximations, Equations (11), (12), and (13), in dealing with varying nadir temperatures and consequently varying scale factors will be evaluated using scaled MARS data in the NWC 6-DOF simulation.

The PCL will require the same type of compensation derived above since it requires the use of a proportional control law for small offsets from the vertical. For large offsets no such compensation is required as the PCL uses the relative order of the antenna output magnitudes to determine the angular velocity commands.

DIRECTION OF COMMANDED ANGULAR VELOCITY VECTOR

One interesting characteristic of the control laws is the difference between the directions of the commanded angular velocity vector and the vector which minimizes the angular rotation required to align the seat with the vertical, assuming the body angular velocity $r = 0$. The direction of the Minimum Rotation Axis (MRA) is found as the cross product of body z axis and the inertial z axis expressed in body axes. Using the standard seat coordinate systems and Euler angles,

$$MRA = \begin{bmatrix} 0 \\ 0 \\ 1 \end{bmatrix} \times C_{B/I} \begin{bmatrix} 0 \\ 0 \\ 1 \end{bmatrix}$$

where $C_{B/I}$ is the Direction Cosine Matrix (DCM) between body and inertial axes. This yields

$$MRA = \begin{bmatrix} -\sin\phi \cos\theta \\ -\sin\theta \\ 0 \end{bmatrix} = \begin{bmatrix} -C_{23} \\ C_{13} \\ 0 \end{bmatrix} \tag{16}$$

where θ and ϕ are the pitch and roll Euler angles of the seat, and C_{13} and C_{23} are components of the DCM. Note that, by definition, C_{13} and C_{23} are the direction cosines between the inertial z axis and the body x and y axes and are therefore equal to the outputs q and p respectively of the ideal DCCL. In order to evaluate the control law outputs, expressions from Reference 2 which provide the

8

angle between each antenna axis and the zenith were used. These expressions are repeated here for convenience.

$$z_1 = \cos^{-1}(\cos\phi\cos\theta)$$
$$z_2 = 90^{o} + \theta \qquad\qquad (17)$$
$$z_3 = \cos^{-1}[(\sin\theta - 3\sin\phi\cos\theta)/2]$$
$$z_4 = \cos^{-1}[(\sin\theta + 3\sin\phi\cos\theta)/2]$$

where z_i is the angle between antenna i and the zenith. The actual antenna outputs are obtained by using the above angles and interpolating the MARS output data for Antenna #1 in Appendix A. A list of the antenna outputs for several seat orientations is given in Table 1. A comparison of the corresponding control law outputs and MRA is presented in Table 2, where the orientations of the commande angular velocity vector and the MRA are the angles from the x body axis of the seat. That is

$$\angle\, MRA = \tan^{-1}\left(\frac{\tan\theta}{\sin\phi}\right) \qquad\qquad (18)$$

from Equation (16), and

$$\angle\, W_c = \tan^{-1}\left(\frac{q}{p}\right) \qquad\qquad (19)$$

from Figure 1.

It should be noted that the data in Table 2 were obtained using the idealized control laws in Equations (9) and (10). None of the previously discussed approximations (Equations (11), (12), and (13)) were used, as the acutal values of A_n and A_z were obtained from Appendix A. Since these quantities cancel in Equation (19) for the HCL and the NHCL, the use of approximations would only affect the data from the MDCCL. The PCL was supplemented with the idealized DCCL to provide proportional control in the appropriate regions.

9

TABLE 1
ANTENNA OUTPUTS FOR SEVERAL
SEAT ORIENTATIONS

θ	ϕ	ANTENNA	z	A
$30°$	$30°$	1	41.4	11.2 MV
		2	120	2.8
		3	97.2	5.1
		4	51.3	10.9
30	60	1	64.3	9.9
		2	120	2.8
		3	113.5	3.3
		4	26	11.3
45	90	1	90	6.4
		2	135	2
		3	105	4.1
		4	15	11.3

TABLE 2
ORIENTATION OF CONTROL LAW
ANGULAR VELOCITY COMMANDS COMPARED
WITH MINIMUM ROTATION AXIS (MRA)

SEAT EULER ANGLES	$\angle$ MRA	$\angle W_c$			
		MDCCL	HCL	MHCL	PCL
$\theta = 30°$ $\phi = 30°$	49.3°	45°	42°	46°	(49.3°)
$\theta = 30$ $\phi = 60$	33.7	30	29	33	53.1
$\theta = 45$ $\phi = 90$	45	40	38	43	54.6

This DCCL, which yields the MRA, was used so that the PCL could
be evaluated independently of errors produced by the other proport-
ional control laws. Evaluation of the data in Table 2 indicates
that the control laws can be ranked in terms of the difference
between their rotation axis and the MRA as follows; closest is
the MHCL, followed by the MDCCL, HCL, and PCL. Although the small
differences between the first three rotation axes are not
presently considered critical, their importance may increase as
the system performance is optimized or if three axis control is
implemented. Also recall that the MDCCL axis will be altered by
the approximations required to implement the un-normalized control
laws. For these reasons the following MHCL was selected for
evaluation using the NWC 6-DOF simulation.

$$p_c = \frac{K \sqrt{3} (A_4 - A_3)}{2 (\hat{A}_z - \bar{A})}$$

$$q_c = \frac{K}{\hat{A}_z - \bar{A}} \left(\frac{A_3 + A_4}{2} - A_2 \right)$$

(20)

where the subscript "c" has been added to indicate commanded values
and K is a constant gain.

12

ADDITIONAL COMPENSATION

Previously the proportional control laws were evaluated by comparing the directions of the commanded angular velocity with a desired direction assuming the body angular velocity r was held to zero. In actuality, these control laws may cause limiting in some component of the system, thus losing their proportional characteristics. Also, r will not be zero. Methods of compensating for these effects are discussed below.

ANGULAR VELOCITY LIMITS

The seat system contains two independent angular velocity feedback control loops which are driven by the control law outputs p_c and q_c. If any portion of this system reaches an operating limit, the proportional characteristics will be lost, resulting in directional divergence of the angular velocity vectors provided by the control law and achieved by the system. One method of preventing this is to limit the maximum values of the angular velocity commands p_c and q_c. Care should be taken in implementing these limits so as to preserve the direction of the commanded angular velocity.

Consider the situation where the angular velocity commands provided by the control law exceed the desired limits as shown in Figure 2. In this case the control law output W_c exceeds the limit for q_c. If q_c is simply limited to W_ℓ and p_c is unchanged, then the axis of the commanded angular velocity will have changed as indicated by ΔW in the figure. Another approach is to preserve the angular velocity axis by changing the command from W_c to W_c'. This can be accomplished as follows, assuming W_ℓ is the desired limit on the control law outputs p_c and q_c.

If
$$q_c > W_\ell > p_c \qquad \text{or} \qquad q_c > p_c > W_\ell$$

let

$$q_c{}' = W_\ell \tag{21}$$

$$p_c{}' = \frac{p_c}{q_c} W_\ell$$

if

$$p_c > W_\ell > q_c \qquad \text{or} \qquad p_c > q_c > W_\ell$$

let

$$p_c{}' = W_\ell$$

$$q_c{}' = \frac{q_c}{p_c} W_\ell \tag{22}$$

But if

$$q_c < W_\ell > p_c$$

then let

$$p_c{}' = p_c$$

$$q_c{}' = q_c \tag{23}$$

where $p_c{}'$ and $q_c{}'$ are the new angular velocity commands after limiting.

W_ℓ = Desired Limits
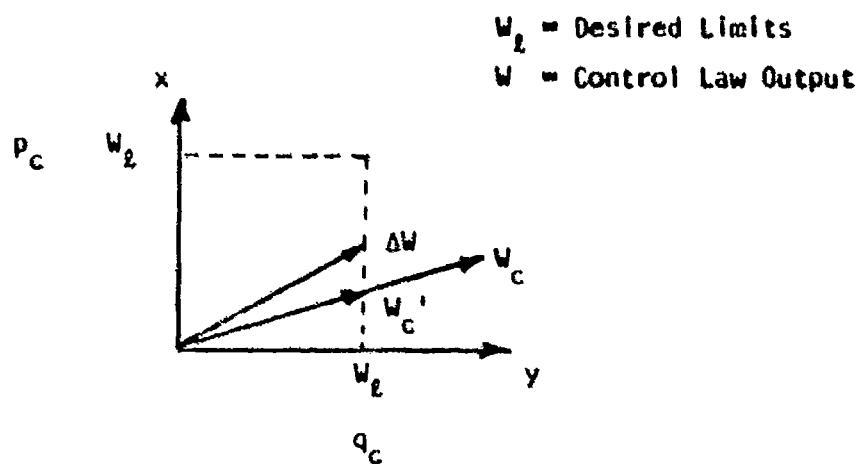
W = Control Law Output

FIGURE 2. Angular Velocity Limits

14

PHASE LAG

The present system provides for control of two of the seat body axis angular velocities p and q. Although the third angular velocity r is not controlled, it is measured and may be used to provide additional compensation. The effects of r on the commanded values of p and q can be visualized using Figure 3. The outputs of the control law p_c and q_c are used to form the commanded angular velocity vector W_c in the x - y plane of the seat body. If r is zero and the control system provides an angular velocity W proportional to W_c, then the direction of W_c will be constant and its magnitude will diminish as the seat approaches its desired attitude. In this case, W and W_c are essentially colinear if the gain and phase characteristics of the two angular velocity feedback control loops are similar, at the frequencies of interest, causing p_c and q_c to be in phase. This is a reasonable assumption as these control loops are similar.
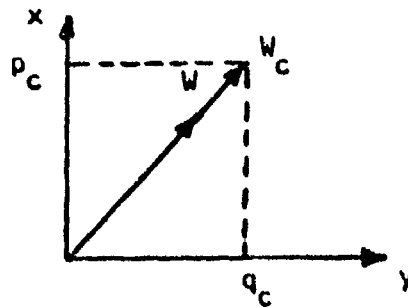
FIGURE 3. Relationship of Angular Velocity and its Commanded Value with r = 0.

However, if r is not zero, W_c will rotate in the x - y plane at an angular frequency which is equal in magnitude but in the opposite direction of r. This rotation introduces a phase shift between p_c and q_c which causes the W and W_c axes to separate as shown in Figure 4. Now W lags W_c by the phase angle ϵ as both vectors rotate in the plane of the figure. If the seat angular velocities p, q and r are well below the bandwidth of angular velocity control loops, then the phase angle ϵ may be reasonably approximated by the

15
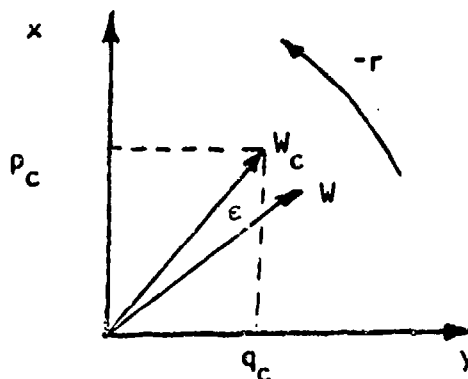
FIGURE 4. Relationship of Angular Velocity and its Commanded Value with $r \neq 0$.

phase angle of the control loop at frequency r. The following low frequency transfer function of this loop was derived in Appendix B.

$$\frac{q}{q_c}(S) = \frac{(0.05\ S + 1)}{(0.1\ S + 1)} \qquad (24)$$

The phase lag at frequency r is

$$\epsilon = \tan^{-1}\left(\frac{.05\ r}{1 + .005\ r^2}\right)$$

If

$$\epsilon \ll 1$$

and

$$.005\ r^2 \ll 1$$

then

$$\epsilon = .05\ r \qquad (25)$$

In order to compensate for this phase angle, modify W_c so that it leads the desired direction of W by ϵ. Now when W lags the

16

modified W_c by ε it, W, will be aligned with its desired direction. This is accomplished using the following transformation

$$\begin{bmatrix} p \\ q \\ r \end{bmatrix}_c^* = \begin{bmatrix} 1 & \varepsilon & 0 \\ -\varepsilon & 1 & 0 \\ 0 & 0 & 1 \end{bmatrix} \begin{bmatrix} p \\ q \\ r \end{bmatrix}_c \tag{26}$$

where $*$ indicates the modified commands. Substituting Equation (25) into (26) yields

$$p_c^* = p_c + .05 \; r \; q_c$$

$$q_c^* = q_c - .05 \; r \; p_c \tag{27}$$

where r is in radians/sec.

It should be noted that, since this compensation was derived for steady state conditions, it will not be exact under other operating conditions.

EVALUATION OF CONTROL LAWS

The MHCL was selected for further evaluation using the NWC 6-DOF digital simulation. Since the scope of this effort did not allow for optimization of the MHCL, some other method was required for determining the gain K in Equation (20). The present angular velocity feedback control loops were designed assuming they were driven by the ideal DCCL. Therefore, a logical approach is to match the gain of the MHCL and the ideal DCCL, for small perturbations from vertical, by proper selection of K. This is accomplished with the aid of the block diagram in Figure 5. For the ideal DCCL

$$K = 1$$

and the effective gain is

$$\frac{K_p}{K_r} = \frac{0.54}{0.09} = 6 \ \frac{rad/sec}{rad} \tag{28}$$

The corresponding gain for the MHCL, calculated using Equation (20) and the MARS data in Appendix C for warmest nadir, is

$$K(2.70)\frac{K_p}{K_r} = K(2.70)\frac{0.54}{0.09} \tag{29}$$

Equating Equations (28) and (29) yields

$$K = 0.37 \tag{30}$$

This value of K was used in Equation (20) and implemented in the simulation as shown in Figure 5. The response of the resulting MHCL was compared with that of the most promising NWC control law. The latter attempts to compensate for scale factor changes by using amplification and limiting with the HCL. Briefly, the strategy here is to use amplification to compensate for low scale factors and use limiting to reduce the resulting overshoot for high scale factors.

The responses of the two control laws for both maximum and minimum scale factors at four different initial attitudes are
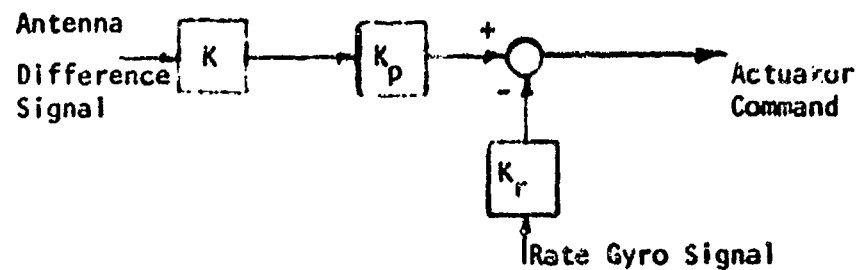
18

FIGURE 5. Block Diagram of MHCL Gain Implementation

summarized in Table 3. Also, the response of the ideal DCCL to
an initial roll error is summarized, Case #1. This case was simu-
lated to provide a reference response in the sense that the angular
velocity loops were designed assuming the use of this control law,
and to facilitate selection of K, Equation (28). Cases #2 through
#9 allow easy comparison of the HCL with amplification and limiting
for conditions of maximum and minimum scale factors. Significant
variations in the time required to come within 3° of the vertical
are apparent in each pair of cases (2-3, 4-5, 6-7, and 8-9). Actual
percentage differences are even greater, because times shown include
approximately 150 msec of time spent on the launch rails, before
any maneuver could begin. Significant variations in the amount of
overshoot are also evident. The initial attitudes of Cases #2 - #9
correspond with those of Cases #10 - #17, which used the MHCL.
Comparison of each pair of these latter cases (10-11, 12-13, 14-15,
and 16-17) reveals much more consistent performance than was
achieved using the HCL with amplification and limiting. A compar-
ison of the control laws at corresponding initial conditions (Cases
2 and 10, 3 and 11, 4 and 12, 5 and 13, 6 and 14, 7 and 15, 8 and
16, and 9 and 17) indicates that the MHCL is slower than the HCL
in reaching the 3° crossover for most cases. However, the former
exhibits less overshoot than the latter in most cases.

The important result of the above comparison is not that
the HCL (with amplification and limiting) is usually faster than
the MHCL, since no attempt was made to optimize the response of

19

TABLE 3
SUMMARY OF CONTROL LAW RESPONSES
OBTAINED FROM THE DIGITAL SIMULATION

CASE	RUN DATE/TIME	CONTROL LAW	ANTENNA SCALE FACTOR	GAIN	INITIAL ATTITUDE	TIME TO 3° CROSSING	OVERSHOOT (DEGS)
1	3/15/80 13:00:27	Ideal DCCL	N/A	-	$\theta = 0°$ $\phi = 70°$	0.68 sec	0.
2	3/14/80 13:05:44	MCL with AMP/LMT	MAX	1.5 X (1.0 limit)	$\theta = 0$ $\phi = 30$	0.44	2.2
3	3/14/80 19:20:21	"	MIN	"	"	0.51	0.36
4	3/14/80 17:16:54	"	MAX	"	$\theta = 0$ $\phi = 70$	0.52	2.7
5	3/14/80 19:20:21	"	MIN	"	"	0.67	0.11
6	3/15/80 12:36:00	"	MAX	"	$\theta = 70$ $\phi = 0$	0.56	4.6
7	3/14/80 19:20:21	"	MIN	"	"	0.75	0.38
8	3/15/80 12:30:00	"	MAX	"	$\theta = 70$ $\phi = 70$	0.59 (PTH) 0.47 (RLL)	4.5 0.4
9	3/14/80 19:20:21	"	MIN	"	"	0.81 (PTH) 0.59 (RLL)	0.16 0.4
10	3/15/80 18:43:55	MMCL	MAX	0.37	$\theta = 0$ $\phi = 30$	0.56	0.
11	"	"	MIN	"	"	0.56	0.
12	"	"	MAX	"	$\theta = 0$ $\phi = 70$	0.75	0.
13	"	"	MIN	"	"	0.75	0.
14	"	"	MAX	"	$\theta = 70$ $\phi = 0$	0.71	0.62
15	"	"	MIN	"	"	0.71	0.65
16	"	"	MAX	"	$\theta = 70$ $\phi = 70$	0.77 (PTH) 0.58 (RLL)	0.29 0.18
17	"	"	MIN	"	"	0.77 (PTH) 0.58 (RLL)	0.30 0.15

NOTE: CATAPULT USED, NO AERO

20

the latter. Rather, the important result is that the MHCL provides comparable responses which are relatively insensitive to scale factor changes. It should be noted that the MHCL responses were obtained with the estimated output of an antenna pointing at the zenith, $\hat{A}_z$ in Equation (20), equal to its actual value in the simulation data. This approximation should not significantly affect the results as only small variations in the zenith temperature are anticipated. If the difference between the estimated and actual zenith temperatures were to become a problem, it might be necessary to update the estimate on-line.

The techniques presented in the section labeled "Additional Compensation" were not evaluated using the 6-DOF simulation.

RECOMMENDATIONS

The previous analysis and evaluation not only establishes the potential of the Modified Heuristic Control Law, Equation (20), for use with the present two-axis control system, but also suggests an increased potential for dealing with more optimal maneuvers which may be desired if a three-axis control system is implemented. As a result, it is recommended that this control law be considered a leading candidate for the MPES/VSS system. This recommendation is made with the knowledge that additional effort is required to provide logic for inverted attitudes and to optimize performance for the range of flight conditions. It is also recommended that the techniques in the section labeled "Additional Compensation" be evaluated for use with a three-axis control system.

FURTHER STUDY

Several areas which appear appropriate for further study are briefly discussed.

An attempt should be made to optimize the control laws for all initial flight conditions. This optimization process should consider such things as probable trajectory of aircraft after ejection, direction of relative wind, maximum maneuvers tolerated by the pilot, and seat attitude and motion at the time of parachute deployment. Also, the techniques presented in the section labeled "Additional Compensation" should be evaluated.

Data should be obtained to determine the MARS output characteristics for measurements over water and along the land-water interface. These data should be used to re-evaluate the candidate control laws.

The number and orientation of the MARS antennas should be analyzed considering the candidate control laws to determine possible advantages of alternate antenna configurations.

Current plans call for testing and evaluation of a three-axis control system. This additional capability will require that the vertical reference system used previously be expanded to an attitude reference system which includes a heading reference. One candidate reference system would use outputs from both the MARS and strapdown rate gyros. Previously, most strapdown systems used the gyro outputs to update a 3 X 3 Direction Cosine Matrix (DCM) which relates the body axes to reference axes. Increasingly popular alternatives to DCM methods include the use of quaternions which are related to Euler parameters. These methods are based on Euler's Theorem which states (in effect) that any rotation of one coordinate system with respect to another may be described by a rotation of some angle about a single fixed axis. The Euler parameters define this rotation angle and axis, and the quaternion is a compact form for representing these parameters. Quaternions offer advantages over the DCM such as increased accuracy and decreased computational requirements, since the former uses only four parameters compared

23

to nine for the latter. Also conditions of nonorthogonality, resulting from computation errors, are much easier to correct for quaternions than for DCM's. The quaternion is ideally suited for the attitude control problem as it defines a rotation axis and angle which will align the body axes with the reference axes. This maneuver is optimal in the sense that it minimizes the total angle through which the body rotates. It is suggested that quaternions be considered for use with future MPES/VSS systems. Quaternions are discussed further in Appendix D.

REFERENCES

1. Code 3921 memo, Reg 3921-62, of 27 June 1979.

2. Code 3273 memo, Ser 3036, of 27 April 1979.

3. Mayo, Ronald A., Relative Quaternion State Transition Relation, AIAA Journal of Guidance and Control, Vol. 2, No. 1, January 1979.

4. Ickes, B. P., A New Method for Performing Digital Control System Attitude Computations Using Quaternions, AIAA Journal, Vol. 8, No. 1, January 1970.

5. Mortensen, R. E., Strapdown Guidance Error Analysis, IEEE Transactions on Aerospace and Electronic Systems, Vol. AES-10, No. 4, July 1974.

APPENDIX A.
MARS OUTPUT DATA

The following data, provided by NWC, were obtained by rolling MARS about its x body axis and recording the outputs corresponding to each antenna. Note that the roll angle is also the angle between Antenna #1 and the zenith.

ROLL ANGLE	#1	ANTENNA #2	OUTPUTS #3	#4
0°	11.310mV	6.435mV	7.013mV	5.552mV
5	11.308mV	6.481mV	6.088mV	6.301mV
10	11.319mV	6.509mV	5.328mV	7.097mV
15	11.324mV	6.468mV	4.632mV	7.719mV
20	11.337mV	6.477mV	3.920mV	8.365mV
25	11.272mV	6.483mV	3.393mV	8.935mV
30	11.227mV	6.482mV	2.921mV	9.402mV
35	11.331mV	6.514mV	2.587mV	9.807mV
40	11.291mV	6.520mV	2.341mV	10.220mV
45	11.164mV	6.491mV	2.120mV	10.470mV
50	10.950mV	6.470mV	1.901mV	10.665mV
55	10.661mV	6.429mV	1.839mV	10.796mV
60	10.207mV	6.375mV	1.769mV	10.901mV
65	9.871mV	6.373mV	1.753mV	10.955mV
70	9.408mV	6.363mV	1.743mV	11.036mV
75	8.811mV	6.353mV	1.807mV	11.102mV
80	7.959mV	6.335mV	1.927mV	11.116mV
85	7.120mV	6.288mV	2.077mV	11.118mV
90	6.362mV	6.286mV	2.210mV	11.127mV
95	5.531mV	6.237mV	2.380mV	11.094mV
100	4.754mV	6.209mV	2.543mV	11.082mV
105	4.094mV	6.179mV	2.606mV	11.045mV
110	3.564mV	6.161mV	2.600mV	11.045mV
115	3.123mV	6.157mV	2.714mV	11.024mV
120	2.788mV	6.145mV	2.671mV	10.909mV
125	2.470mV	6.094mV	2.350mV	10.860mV
130	2.265mV	6.108mV	2.523mV	10.859mV
135	2.084mV	6.121mV	2.552mV	10.712mV
140	1.961mV	6.113mV	2.637mV	10.565mV
145	1.850mV	6.070mV	2.692mV	10.333mV
150	1.843mV	6.054mV	2.929mV	10.114mV
155	1.832mV	6.035mV	3.279mV	9.757mV
160	1.813mV	6.022mV	3.652mV	9.313mV
165	1.779mV	5.965mV	4.040mV	8.811mV
170	1.739mV	5.949mV	4.556mV	8.170mV
175	1.733mV	5.938mV	5.214mV	7.518mV
180	1.721mV	5.913mV	5.803mV	6.832mV

APPENDIX B.
DERIVATION OF ANGULAR VELOCITY CONTROL LOOP
LOW FREQUENCY TRANSFER FUNCTION

A block diagram of the control loop was obtained from NWC and
reduced to that shown in Figure B-1 by neglecting the transfer
functions of the rate gyro, filter circuit, and part of the actuator.
The closed-loop transfer function of this system is

$$\frac{\dot{q}}{\dot{q}_c} (S) = \frac{3266 \ (S + 20)}{S^3 + 131 \ S^2 + 6416 \ S + 65320} \qquad (B-1)$$

The roots of the characteristic equation are found using spectral
separation. At high frequencies $S \gg 1$ and therefore the constant
term is neglected and the poles are the roots of

$$S^2 + 131 + 6416 = 0$$

or

$$S = -66 \pm 461 \qquad \qquad , \quad (B-2)$$

at low frequencies $S \ll 1$ and therefore the poles are the roots of

$$6416 \ S + 65320 = 0$$

or

$$S \approx -10 \qquad (B-3)$$

The roots of the characteristic equation are approximately the values
given in Equations (B-2) and (B-3). Since the roots of Equation
(B-2) are significantly "faster" than that of Equation (B-3), the
former were neglected in obtaining the following low frequency
transfer function.

$$\frac{\dot{q}}{\dot{q}_c} (S) \approx \frac{3266 \ (S + 20)}{6416 \ S + 65320}$$

$$\approx \frac{0.05 \ S + 1}{0.1 \ S + 1} \qquad (B-4)$$
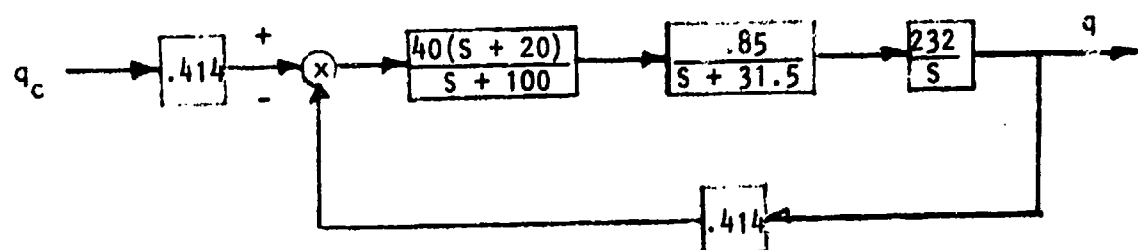
27

FIGURE B-1. Block Diagram of Low Frequency Transfer Functions
in Angular Velocity Control Loop.

28

APPENDIX C.
SCALING OF MARS OUTPUT DATA

The NWC 6-DOF digital simulation accommodates three different
sets of MARS data which relate the angle between the nadir and an
antenna to the sensed temperature and, therefore, to an output
signal. The data sets, which correspond to the warmest, nominal,
and coolest expected nadir temperatures, are obtained by scaling
the data for Antenna #1 in Appendix A. A sketch of the resulting
data is shown in Figure C-1. Note that the independent variable
(abscissa) has been changed to the angle from the nadir, in order
to be consistent with the 6-DOF simulation. The scaling was
accomplished assuming the data in Appendix A correspond to zenith
and nadir temperatures of 15°K and 250°K, respectively. Also,
the nominal and minimum nadir temperatures are assumed to be 200°K
and 150°K, respectively. The scaled data set for the warmest
nadir surface was obtained by normalizing the Antenna #1 data in
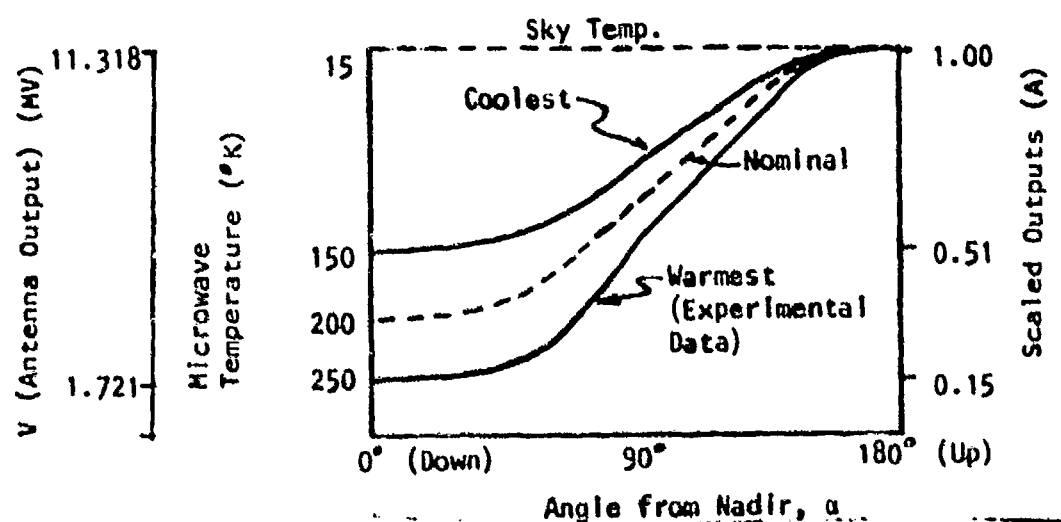Appendix A to the zenith value, 11.318 MV.

FIGURE C-1.   Sketch of Scaled Output Data

29

The temperature differences between the zenith and both the coolest and nominal nadir surfaces

$$\Delta T_c = 150^\circ - 15^\circ = 135^\circ K$$

$$\Delta T_n = 200^\circ - 15^\circ = 185^\circ K$$

were then divided by the assumed difference for the warmest nadir surface

$$\Delta T_w = 250^\circ - 15^\circ = 235^\circ K$$

Finally, the resulting proportionality constants were used to scale the antenna output voltage for the warmest nadir, in order to obtain data sets for the nominal and coolest nadirs, as follows

$$A_n (\alpha) = \frac{1}{V(180^\circ)} \left[V(180^\circ) - \frac{\Delta T_n}{\Delta T_w} \left(V(180^\circ) - V_w (\alpha) \right) \right]$$

and

$$A_c (\alpha) = \frac{1}{V(180^\circ)} \left[V(180^\circ) - \frac{\Delta T_c}{\Delta T_w} \left(V(180^\circ) - V_w (\alpha) \right) \right]$$

where

$A_n (\alpha)$ = Scaled data for nominal surface

$A_c (\alpha)$ = Scaled data for coolest surface

$V_w (\alpha)$ = Antenna output for warmest nadir conditions, MV

$V(180^\circ)$ = Output of antenna pointing at zenith, MV. (Assumed the same for all nadir temperatures)

α = Angle from antenna axis to nadir

The resulting data sets are shown in Table C-1.

30

TABLE C-1
MARS DATA SETS USED
IN NWC 6-DOF SIMULATION

α (ANGLE FROM NADIR)	ANTENNA OUTPUT VOLTAGE (MV)	SCALED DATA SETS		
		WARMEST	NOMINAL	COOLEST
180°	11.318	1.00	1.00	1.00
175	11.308	1.00	1.00	1.00
170	11.319	1.00	1.00	1.00
165	11.324	1.00	1.00	1.00
160	11.337	1.00	1.00	1.00
155	11.272	1.00	1.00	1.00
150	11.227	0.99	0.99	1.00
145	11.331	1.00	1.00	1.00
140	11.291	1.00	1.00	1.00
135	11.164	0.99	0.99	0.99
130	10.958	.97	.97	.98
125	10.661	.94	.95	.97
120	10.287	.91	.93	.95
115	9.871	.87	.90	.93
110	9.408	.83	.87	.90
105	8.811	.78	.83	.87
100	7.959	.70	.77	.83
95	7.120	.63	.71	.79
90	6.362	.56	.66	.75
85	5.531	.49	.60	.71
80	4.754	.42	.54	.67
75	4.094	.36	.50	.63
70	3.564	.31	.46	.61
65	3.123	.28	.43	.58
60	2.788	.25	.41	.57
55	2.470	.22	.38	.55
50	2.265	.20	.37	.54
45	2.084	.18	.36	.53
40	1.961	.17	.35	.53
35	1.850	.16	.34	.52
30	1.843	.16	.34	.53
25	1.832	.16	.34	.52
20	1.813	.16	.34	.52
15	1.779	.16	.34	.52
10	1.739	.15	.33	.51
5	1.733	.15	.33	.51
0	1.721	.15	.33	.51

APPENDIX D.
ATTITUDE CONTROL USING QUATERNIONS

One method of describing the relationship between two coordinate frames is the 3 X 3 Direction Cosine Matrix (DCM). Many strapdown systems use rate gyro outputs to update the DCM, thereby maintaining an attitude reference. An advantage of this method is that the matrix required to transform vectors between the coordinate systems, that is the DCM, is available directly. An alternate method of describing orientation involves the use of quaternions. This method is based on Euler's Theorem which states (in effect) that any rotation of one coordinate system with respect to another may be described by a rotation α about a fixed axis $\hat{E}$. In one form, the quaternion presents this rotation as a four component vector, Reference 3.

$$Q = \begin{bmatrix} q_1 \\ q_2 \\ q_3 \\ q_4 \end{bmatrix} = \begin{bmatrix} \cos \frac{\alpha}{2} \\ E_x \sin \frac{\alpha}{2} \\ E_y \sin \frac{\alpha}{2} \\ E_z \sin \frac{\alpha}{2} \end{bmatrix} \qquad (D\text{-}1)$$

where the unit vector

$$\hat{E} = \begin{bmatrix} E_x \\ E_y \\ E_z \end{bmatrix} \qquad (D\text{-}2)$$

The components of Q are referred to as the Euler symmetric parameters and were chosen to simplify computations of successive rotations, Reference 4. Note that these components satisfy the normality condition

$$q_1^2 + q_2^2 + q_3^2 + q_4^2 = 1 \qquad (D\text{-}3)$$

32

One method of combining quaternions to describe successive rotations involves the use of matrix notation. Consider three coordinate systems a, b, and c. If the quaternion Q_{ba} describes the rotation of a into b, and the quaternion Q_{cb} describes the rotation of b into c, then the rotation of a into c is described by the quaternion (Reference 4)

$$Q_{ca} = \underbrace{\begin{bmatrix} q_1 & -q_2 & -q_3 & -q_4 \\ q_2 & q_1 & -q_4 & q_3 \\ q_3 & q_4 & q_1 & -q_2 \\ q_4 & -q_3 & q_2 & q_1 \end{bmatrix}}_{\text{Components of } Q_{cb}} Q_{ba} \qquad (D-4)$$

An attitude reference can be maintained by updating a quaternion describing the relationship between inertial and body axes using the differential equation (Reference 5)

$$\dot{Q}(t) = \frac{1}{2} \begin{bmatrix} 0 & -p & -q & -r \\ p & 0 & r & -q \\ q & -r & 0 & p \\ r & q & -p & 0 \end{bmatrix} Q(t) \qquad (D-5)$$

where p, q, and r are the body angular velocities obtained from strapdown rate gyros.

The above equations define and describe some properties of a quaternion represented as a four component vector. Some advantages of quaternions over the DCM for use in attitude reference systems are now discussed. First, the quaternion contains four components and is therefore only once redundant, whereas the DCM contains nine elements and is therefore six times redundant. Second, computation errors entering into the DCM require normalization and orthogonalization of three vectors. The latter process can be difficult. The corresponding errors in a quaternion merely require normalization

33

to satisfy the condition of Equation (D-3). Third, successive
rotations using DCM's require multiplication of two 3 X 3 matrices,
which leads to 27 multiplications and 18 additions, compared with
16 multiplications and 12 additions for the same operation using
quaternions, Equation (D-4). Fourth, the strapdown differential
equation for a DCM requires 18 multiplications and 9 additions,
compared with 12 and 8 respectively for quaternions, Equation (D-5).
For systems which require the transformation of vectors between
inertial and body axes, the above computational advantages of quat-
ernions may be lost when the DCM is calculated from the quaternion.
However, most attitude control systems do not require direct vector
transformations and, therefore, do not require explicit knowledge
of the DCM. In these cases the quaternion retains its computational
advantages.

Another advantage of quaternions is that they explicitly define
a single rotation axis and angle which will result in alignment of
the inertial and body coordinate systems. If the angular velocity
vector is along this axis, the resulting maneuver will be optimum
in the minimum angle sense. Therefore, a logical approach is to
define angular velocity commands in terms of the quaternion para-
meters. Possibilities include

$$
\begin{bmatrix} p \\ q \\ r \end{bmatrix}_c = K \begin{bmatrix} q_2 \\ q_3 \\ q_4 \end{bmatrix}
\tag{D-6}
$$

or

$$
\begin{bmatrix} p \\ q \\ r \end{bmatrix} = K \begin{bmatrix} aE_x \\ aE_y \\ aE_z \end{bmatrix}
\tag{D-7}
$$

where the subscript c indicates commanded values and K is a constant
gain.

Initialization of the quaternion or DCM is required if either
is used in a strapdown attitude reference/control system. For

34

3-axis control of the MPES/VSS escape system it is desired to use
the MARS sensor to perform this initialization. This approach is
complicated by the limitations of the MARS outputs. Previous
analysis has shown that MARS can provide a reference to the vertical,
however, it has not indicated how to extract (changes in) yaw
attitude. Therefore, yaw attitude must be referenced to its initial
value, and changes from this value should either be calculated using
the rate gyro outputs or minimized by proper selection of the
commanded angular velocity. One method of accomplishing the latter
is to estimate the pitch and roll angles using the MARS outputs,
form quaternions for first returning the roll attitude to zero
and then returning the pitch attitude to zero, and use Equation
(D-4) to calculate the quaternion for these successive rotations.
This resulting quaternion defines a single axis rotation which
will align the seat with the vertical without changing its heading.
This initialized quaternion can be propagated by numerical inte-
gration of Equation (D-5) and a control law similar to those in
Equations (D-6) and (D-7) can then be used. A second method is
to estimate the minimum rotation axis and angle to the vertical
using the MARS outputs, form the corresponding quaternion and
determine the associated heading change, form a quaternion to
return the heading to its original value, and calculate the quat-
ernion for these successive rotations. This quaternion should
correspond to that obtained using the previous method and, therefore
can be used in the same manner.

In the approaches discussed above the MARS outputs were only
used to initialize a quaternion. An alternate approach is to also
use the MARS outputs to update the attitude estimate at given time
intervals along the trajectory. A standard approach to this problem
of combining attitude and angular velocity data is to use a steady-
state Kalman filter.

For some flight conditions, limited control authority may make
it undesirable to command an angular velocity along the "quaternion
axis." In these cases the original quaternion can be propagated
and a modified quaternion used for control. At a later point along

35

the trajectory, control can be switched to the original quaternion which will provide an optimum maneuver to the vertical and original heading. The modified quaternion, mentioned above, may result from simple changes to the original or may result from a successive rotation calculation, depending on the desired control strategy.

The above methods of using the MARS outputs to initialize quaternions should be evaluated with respect to their relative accuracies and ease of implementation in a microprocessor. Also, advantages of using the MARS outputs to update the seat attitude should be evaluated. Finally, modified quaternion control laws should be formulated and their effectiveness in dealing with limited control authority evaluated. These evaluations should include the use of suitable simplifying approximations.